

Atomistic Wear in a Single Asperity Sliding Contact

Bernd Gotsmann and Mark A. Lantz

IBM Research GmbH, Zurich Research Laboratory, 8803 Rüschlikon, Switzerland

(Received 18 June 2008; published 16 September 2008)

Abrasive wear of sharp silicon tips sliding distances of up to 750 m on a polymeric surface is studied using atomic force microscopy. The data cannot be explained by conventional macroscopic wear models. We present a new model in which the barrier for breaking an atomic bond is lowered by the frictional stress acting on the contact. Quantitative agreement is obtained between the model and wear data for all load forces and sliding distances studied.

DOI: [10.1103/PhysRevLett.101.125501](https://doi.org/10.1103/PhysRevLett.101.125501)

PACS numbers: 62.20.Qp, 07.79.Lh

Understanding the basic mechanisms of friction and wear has been a long-standing open question. This is surprising when one considers the long history of enquiry into the subject and the deceptively simple empirical laws describing macroscopic tribological phenomena: Friction is simply proportional to load (Amonton's law) and wear volume is proportional to load and sliding distance (Archard's wear law), and both laws are independent of contact area and velocity. Although broadly applicable on the macroscopic scale, the underlying mechanisms remain unclear.

One of the reasons that a deeper understanding of the underlying mechanisms has proved so elusive is the complex nature of the contact between two macroscopic bodies. On the nanometer scale, engineering surfaces are rough, and mechanical contact occurs mostly between the asperities of the surfaces. There is thus a discrepancy between the apparent contact area referred to by Amonton and the real contact area.

The atomic force microscope (AFM) is ideally suited to gain insight into the problem as it allows the behavior of a *single* asperity to be studied. This simplification has led to recent progress in understanding friction, showing, for example, that single-asperity friction does not always follow Amonton's law, but in some cases friction is proportional to the real contact area [1,2]. This apparent discrepancy between a single asperity and real engineering contacts was resolved by Greenwood and Williamson [3], who showed that for randomly rough surfaces the real area of contact varies with the applied load, and hence Amonton's law is recovered. Such progress in the study of nanoscale friction has not been paralleled in the area of nanoscale wear. In fact, many AFM friction experiments are described as operating in a "wearless" regime, i.e., with a wear rate below the detection limit of the experiment. Such low wear rates make it difficult to quantify wear.

Here we report a study into the nature of single-asperity wear of sharp silicon tips sliding on flat polymer surfaces. The silicon tip on polymer surface serves as an excellent model system of wear, and is also technologically relevant due to the emergence of scanning-probe-based data storage

[4,5] and nanolithography [6]. We quantify tip wear *in situ* as a function of sliding distance for applied loads ranging from 5 to 100 nN. In contrast to previous nanotribology work, we study extremely large sliding distances of up to 750 m, a requirement for the practical implementation of AFM-based data storage and lithography. We propose a mechanism that describes wear as a thermally activated atom-by-atom loss process resulting from a lowering of the barrier to remove an atom due to the stretching of atomic bonds by frictional shear stress. From this, a wear model is developed that quantitatively describes our data for the entire range of applied loads and sliding distances studied.

The wear experiments were performed using a home-built AFM and compliant (0.15 N/m) silicon cantilevers [7] with tips that we assume were initially covered with a 2–3 nm native oxide. The AFM is housed in a vacuum chamber to facilitate control of the experimental environment. Prior to each experiment, the chamber was baked and pumped to high vacuum and then vented with dry, high-purity nitrogen or dry air (<2 ppm H₂O). As a countersurface, we used a 100-nm film (roughness ≈ 0.4 nm_{rms}) of cross-linked polyaryletherketone spun cast on silicon. The material was chosen for its technical relevance to AFM data-storage applications [4,5]. In all of the experiments presented here, the polymer does not show significant signs of wear. Tip-wear experiments were performed by raster scanning a tip over a 30 μ m \times 6 μ m area of the sample in constant-height mode, i.e., without fast z feedback, and without the acquisition of image data, to facilitate the use of high scan speeds. To minimize load variation to ≤ 3 nN, the tip was scanned parallel to the predetermined plane of the sample surface. The fast-scan axis (mean velocity of 1.5 mm/s) was driven with a sinusoidal waveform to prevent ringing of the scanner. Normal-force versus displacement curves were taken every 62 cm (i.e., 41 s) of sliding to provide slow feedback control of the load force and to monitor the state of the tip as described below. After every 62 cm of sliding, a reduced scan velocity was used to acquire an image of the area in which the fast sliding had been performed, to monitor the state of the polymer surface.

In many previous AFM tip-wear studies, wear was characterized using electron microscopy [8–11] or a sharp tip was used to image the blunted tip [12–14] at the end of the wear experiment, providing a single value of wear volume and a measure of the average wear rate, or a few values of wear volume measured by interrupting the experiment. Ideally, in order to gain more insight into the wear process, we would like to monitor tip abrasion in a quasicontinuous manner during the experiment. To achieve this, we use the tip-sample adhesion as a measure of the tip-sample contact geometry. The adhesion depends on the tip and sample materials (which are constant in this study) and the geometry of the tip. Because of the dry conditions applied, meniscus forces do not play a role. Before and after each experiment, the geometry of the tip apex was characterized using scanning electron microscopy (SEM). Initially, the tips were extremely sharp and well modeled by a cone with a spherical cap having a radius of 3–5 nm. After a few meters of sliding, the spherical cap is worn away and the tip can be modeled as a truncated cone. For this flat punch geometry, the decohesion (pulloff) force F_{adh} is proportional [15] to the radius of the flat end a : $F_{\text{adh}} = k_{\text{adh}}a$. This assumption can be verified by comparing the value of k_{adh} calculated from the adhesion force and the radius of the flattened tip measured at the end of an experiment. For the 11 tips analyzed in this study with final tip radii between 10 and 50 nm, we obtained $k_{\text{adh}} = 4.6 \pm 0.9$ N/m. The scatter is within the experimental uncertainty in the adhesion force measurement.

Figure 1 shows an example of a typical wear test performed with an applied load of 5 nN in a dry environment (artificial air [16]) and a sliding distance of 750 m. After the wear test, a wear volume of 1.5×10^4 nm³ was determined from preexperiment [Fig. 1(a)] and postexperiment [Fig. 1(b)] SEM images. Figure 1(c) shows the adhesion data acquired during the experiment that has been con-

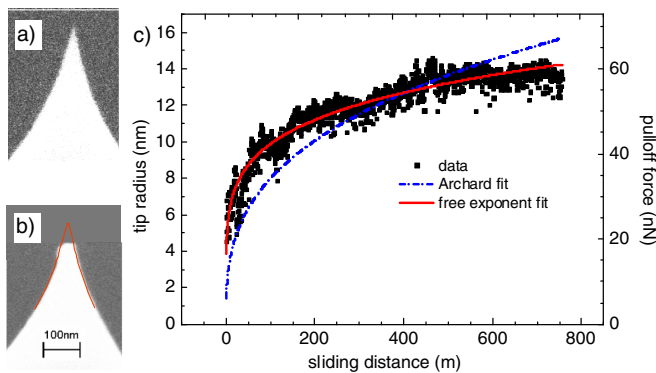


FIG. 1 (color online). Wear data for a tip sliding on a polymer surface with a load force of 5 nN: (a) SEM image of the tip before and (b) after testing. A contour of the fresh tip is overlaid to visualize the volume loss (1.5×10^4 nm³). (c) Plot of adhesion force and contact radius versus sliding distance. The data are fitted using Eq. (1) with $m = 1/3$ (corresponding to Archard's wear law) and a fit with free m yielding $m = 0.18$.

verted into radius versus sliding distance using $F_{\text{adh}} = k_{\text{adh}}a$ in combination with the radius and adhesion force measured at the end of the experiment. In this experiment, initially the adhesion increases rapidly, roughly doubling within the first few meters of sliding, followed by a continuous decrease of the rate of change in adhesion. To gain more insight into the wear process, we systematically studied the influence of sliding distance and pressure by performing experiments with applied loads ranging from 5 to 100 nN. Representative examples of the tip radius versus sliding distance data are shown in Fig. 2.

We first fit Archard's wear model to the data, i.e., wear volume V proportional to load force F_N and sliding distance d , $V = kF_N d$, where k is a constant. Applying this model to our conical tip geometry and solving for the radius a of the flattened end results in

$$a \propto d^m F_N^n, \quad (1)$$

with $m = n = 1/3$. The dash-dotted line in Fig. 1 is a least-squares fit of this relation to the data illustrating

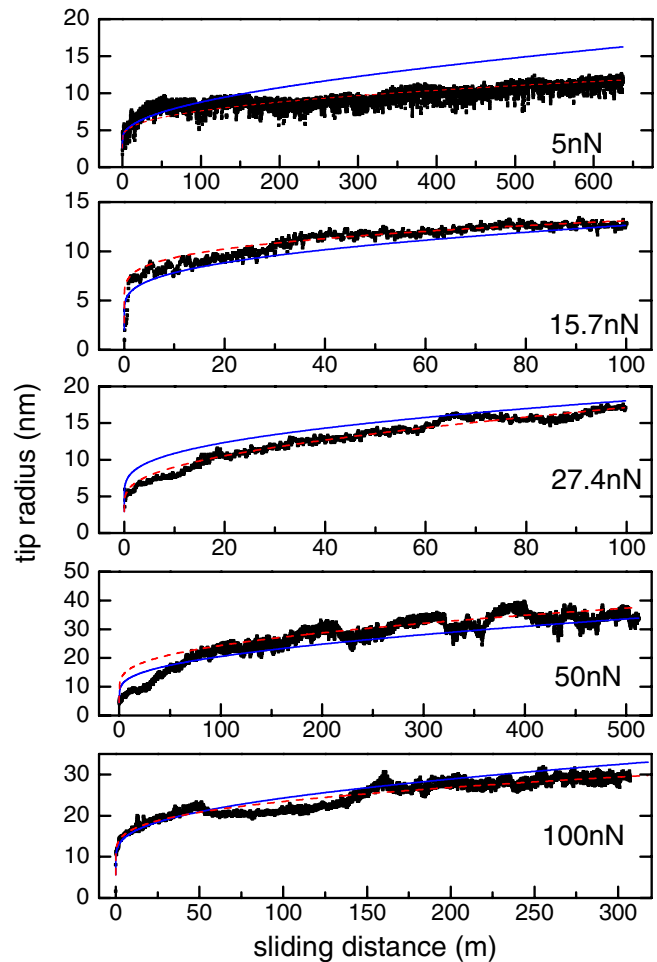


FIG. 2 (color online). Wear data and fits for representative experimental runs between 5 and 100 nN load force. Individual fits (dashed lines) and fits with the same parameters (solid lines), using $E_{\text{eff}} = 0.983$ eV and $\xi V_{aN} = 5.5 \times 10^{-29}$ m³ are plotted.

that Archard's law does not fit the data. Similarly poor-quality fits were obtained for the data of Fig. 2. We find that generally our data cannot be well fitted using a single exponent as in Eq. (1), and best fits tend to yield $m < 1/3$. Previously, Maw *et al.* and Chung *et al.* also reported that their AFM wear data are not well fitted by Archard's law [8–10,13], indicating that Archard's law is not generally applicable to nanoscale wear. The situation appears analogous to friction, where macroscopic friction laws fail on the nanoscale [17,18].

Comparing all of the data sets presented in Figs. 1 and 2, we note that there are several features that provide insight into the wear process. First, the wear rates in general are low. For example, for the data of Fig. 1, the average wear rate roughly corresponds to the loss of one atom per micron of sliding. Second, wear proceeds as a smooth process, without indication of fracture. Third, the wear rate increases with increasing applied load, and decreases at large sliding distance.

The first two observations imply that wear occurs through an atom-by-atom loss process, which in turn implies the breaking of individual bonds. Such bond breaking can be described by a thermally activated process governed by Arrhenius kinetics. Using this approach, the height loss rate $\partial h/\partial t$ of the tip is described as

$$\partial h/\partial t = b f_a \exp(-E_a/(k_B T)), \quad (2)$$

with f_a and b being the attempt frequency and lattice parameter, respectively. E_a is an activation energy, k_B Boltzmann's constant, and T the absolute temperature.

To explain the third observation, we argue that the activation barrier E_a is reduced through bond stretching by the shear stress τ acting on the bonds. In its simplest form, the reduction is proportional to the shear stress $E_a - V_a \tau$ with a constant V_a . V_a is called the activation volume and is an empirical material property without direct correspondence to real space.

A similar mechanism has previously been proposed in the context of nanoscale wear of surfaces under the influence of an AFM tip [18–22]. In surface wear the rearranging and recrystallization of removed atoms may be observed [23] and complicates the analysis. In our case, the abraded atoms distribute or diffuse away sufficiently quickly on the countersurface and therefore Eq. (2) is valid [19]. To fully explain tip wear, however, Eq. (2) (with reduced activation energy) is not sufficient for two reasons. First, according to Eq. (2) wear is a function of contact time and not sliding distance [18]. Second, for the case of tip wear and not surface wear, we have to assume that τ varies as a function of tip blunting. We therefore develop the model further by incorporating the assumption that τ results from the lateral, frictional stress at the interface, and that τ is a function of the pressure acting on the contact and sliding velocity. Thus, as the contact area increases through wear, the pressure acting on the tip decreases, reducing the

shear force acting on each tip atom at the interface and hence resulting in a decrease in wear rate.

Following the analysis by Briscoe and Evans [24], the dependence of the shear stress on normal pressure $F_N/(\pi a^2)$ and velocity v is assumed to be

$$\tau = \tau_0 + \xi F_N/(\pi a^2) + (k_B T/V_a) \ln(v/v_0), \quad (3)$$

where τ_0 , ξ , and v_0 are constants [25]. The normal load F_N is given by the applied and the adhesive forces $F_N = F_{\text{appl}} + F_{\text{adh}}$. Equation (3) has been experimentally validated for several different tip-sample systems [18,24,28].

To proceed, we relate Eq. (2) to the sliding distance d using the velocity $v = \partial d/\partial t$, and tip height h is replaced by the tip radius a . For a conical tip with opening angle θ , the instantaneous “wear rate” is given by

$$\begin{aligned} \partial a(d)/\partial d &= \tan(\theta)(f_a b/v_0) \\ &\times \exp\left[\frac{-E_a}{k_B T} + \frac{V_a}{k_B T} \left(\tau_0 + \xi \frac{F_{\text{appl}} + k_{\text{adh}} a}{\pi a^2}\right)\right]. \end{aligned} \quad (4)$$

Figure 3 shows a numerical solution of Eq. (4). Three distinct regimes can be identified in the figure. Initially (i), a small slope is observed in the $\log(a)$ - $\log(d)$ relation. The slope is approximately constant and corresponds to a small exponent m in Eq. (1). In this regime, the tip is rapidly blunted, and the wear rate depends strongly on load force but only weakly on the constant part of the activation energy, $E_{\text{eff}} = E_a - V_a \tau_0$. This is because the change in

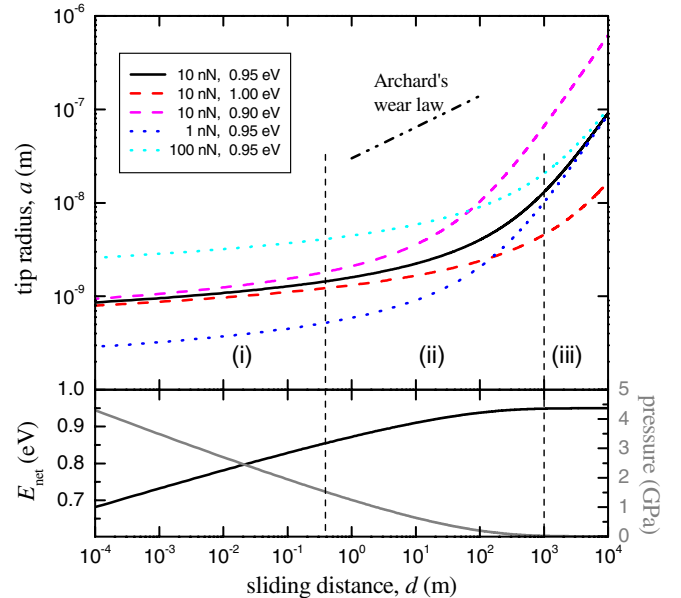


FIG. 3 (color online). Wear modeled using Eq. (4) using $F_N = 10$ nN, $E_{\text{eff}} = E_a - V_a \tau_0 = 0.95$ eV, and $\xi V_a = 10^{-29}$ m³ (solid lines). The dotted lines correspond to 0.95 eV and load forces 1 and 100 nN. The dashed lines correspond to 10 nN and $E_{\text{eff}} = 0.9$ and 1.0 eV. The slope of Archard's wear law is plotted in the dash-dotted line.

activation energy is largely driven by the pressure under the tip.

Region (ii) is particularly important for interpreting previously reported nanoscale wear data. In this region the exponent m transitions from ≈ 0 to 1 over several orders of magnitude of d . The change of slope is controlled by a continuous change of pressure under the tip and consequently a change of the net activation barrier $E_{\text{net}} = E_a - V_a\tau$. Thus, for small sliding distance wear tests, a fit using a single exponent m may be possible, and under certain conditions Archard's wear law may be a good approximation.

In the third regime (iii), the wear behavior asymptotically becomes independent of pressure and is strongly affected by the effective energy barrier E_{eff} . In this region, the normal pressure is too small to contribute to the wear rate and Eq. (4) can be approximated as

$$a = \left[\tan(\phi) \frac{f_a b}{v_0} \exp\left(\frac{-E_a + \tau_0 V_a}{k_B T}\right) \right] d. \quad (5)$$

In order to apply the model to the experimental data of Fig. 2, we replace the relationship $a = h \tan(\theta)$ for a perfect cone with a function $a(h)$ that includes an initial tip shape with a rounded apex as characterized using SEM. Not all parameters in Eq. (4) are independent. Fixing the uncritical parameters with typical values of the phonon frequency $f_a = 10^{12} \text{ s}^{-1}$, and lattice spacing $b = 4 \times 10^{-10} \text{ m}$, and $v_0 = 1 \text{ m/s}$, we use the effective barrier $E_{\text{eff}} = E_a - V_a\tau_0$, and $V_{aN} = \xi V_a$ as a fit parameters.

Figure 2 shows five representative examples (out of 10 data sets fitted). Individual least-squares fits lead to E_{eff} with a strikingly low standard deviation of 4% around 0.96 eV. V_{aN} is influenced more by experimental errors and yields values between 10^{-29} and $1.5 \times 10^{-28} \text{ m}^3$ [29]. As E_{eff} and V_{aN} are not orthogonal, a simultaneous least-squares fit (solid lines) of all data sets yields a slightly different $E_{\text{eff}} = 0.983 \text{ eV}$ and $V_{aN} = 5.5 \times 10^{-29} \text{ m}^3$. In both cases, the magnitude of the fit parameters is consistent with the assumption of breaking individual bonds.

The good agreement obtained between the model and experimental data provides a strong validation of the model. The model provides insight into nanoscale wear, and allows tip lifetime predictions to be made for emerging probe technologies.

We thank the ZRL probe storage team and gratefully acknowledge helpful discussions with R. Cannara, R. Carpick, D. Jubin, U.D. Schwarz, and, in particular, U. Duerig. Further thanks go to M. Despont and U. Drechsler for the tips, and to R. Pratt and J. Hedrick for the polymer samples.

-
- [1] M. A. Lantz, S. J. O'Shea, M. E. Welland, and K. L. Johnson, *Phys. Rev. B* **55**, 10776 (1997).
 [2] R. W. Carpick, D. F. Ogletree, and M. Salmeron, *Appl. Phys. Lett.* **70**, 1548 (1997).

- [3] J. A. Greenwood and J. B. P. Williamson, *Proc. R. Soc. A* **295**, 300 (1966).
 [4] P. Vettiger *et al.*, *IEEE Trans. Nanotechnol.* **1**, 39 (2002).
 [5] E. Eleftheriou *et al.*, *IEEE Trans. Magn.* **39**, 938 (2003).
 [6] B. Gotsmann, U. Duerig, J. Frommer, and C. J. Hawker, *Adv. Funct. Mater.* **16**, 1499 (2006).
 [7] M. Despont *et al.*, *Sens. Actuators A, Phys.* **80**, 100 (2000).
 [8] K.-H. Chung and D.-E. Kim, *Tribol. Lett.* **15**, 135 (2003).
 [9] K.-H. Chung, Y.-H. Lee, and D.-E. Kim, *Ultramicroscopy* **102**, 161 (2005).
 [10] K.-H. Chung *et al.*, *IEEE Trans. Magn.* **41**, 849 (2005).
 [11] R. H. Geiss, M. Kopycinska-Mueller, and D. C. Hurley, *Microsc. Microanal.* **11**, 364 (2005).
 [12] A. G. Khushudov, K. Kato, and H. Koide, *Tribol. Lett.* **2**, 345 (1996).
 [13] W. Maw, F. Stevens, S. C. Langford, and J. T. Dickinson, *J. Appl. Phys.* **92**, 5103 (2002).
 [14] B. Bhushan and K.-J. Kwak, *Appl. Phys. Lett.* **91**, 163113 (2007).
 [15] D. Maugis, *J. Colloid Interface Sci.* **150**, 243 (1992).
 [16] All other experiments described in this Letter were obtained under a nitrogen atmosphere. No difference in wear behavior between dry air versus pure nitrogen was detected.
 [17] B. Bhushan, *Nanotribology and Nanomechanics* (Springer, Berlin, 2005).
 [18] *Fundamentals of Friction and Wear on the Nanoscale*, edited by E. Gnecco and E. Meyer (Springer, Berlin, 2007).
 [19] M. d'Accunto, *Tribol. Int.* **36**, 553 (2003).
 [20] M. d'Accunto, *Nanotechnology* **15**, 795 (2004).
 [21] M. d'Accunto, *Nanotechnology* **17**, 2954 (2006).
 [22] S. Kopta and M. Salmeron, *J. Chem. Phys.* **113**, 8249 (2000).
 [23] E. Gnecco, R. Bennewitz, and E. Meyer, *Phys. Rev. Lett.* **88**, 215501 (2002).
 [24] B. J. Briscoe and D. C. B. Evans, *Proc. R. Soc. A* **380**, 389 (1982).
 [25] The term $\xi F_N / (\pi a^2)$ implies that pressure variations across the contact area do not play a role. Any local pressure variation induces local variations of the wear rate across the tip diameter, and a finite tip curvature will be attained asymptotically. To understand this, consider both extremes. For a spherical tip, the pressure maximum is in the center [26], leading to a flattening of the tip. For a flat punch, the maximum pressure is at the periphery leading to a curved tip. Asymptotic shapes computed for Archard's wear law [27] are close to a flat punch.
 [26] K. L. Johnson, *Contact Mechanics* (Cambridge University Press, Cambridge, England, 1985).
 [27] I. G. Goryacheva, *Contact Mechanics in Tribology* (Kluwer Academic, Dordrecht, 1998).
 [28] N. S. Tambe and B. Bhushan, *Nanotechnology* **16**, 2309 (2005).
 [29] The worst fit is for the lowest applied load. This may result because the relative uncertainty in the applied load is the largest in this case or may indicate an additional dependence of V_{aN} on pressure.